Anomalous Melting Transition of the Charge-Ordered State in Manganites

C. H. Chen,[1] S. Mori,[2] and S-W. Cheong[1,3]
[1]*Bell Laboratories, Lucent Technologies, Murray Hill, New Jersey 07974*
[2]*Department of Physics, Tokyo Institute of Technology, Meguro-ku, Tokyo, Japan*
[3]*Department of Physics and Astronomy, Rutgers University, Piscataway, New Jersey 08855*
(Received 24 May 1999)

Melting of the charge-ordered state in $(La, Ca)MnO_3$ and $(Pr, Ca)MnO_3$ is characterized by an anomalously large decrease of the wave vector—as much as 25% through the transition. High resolution lattice images obtained from electron microscopy reveal that the large change occurs as a result of formation of new clusters with charge-ordering modulation wavelength increased by integral lattice parameter. Our findings can be attributed to the discrete nature of the charge ordering on the manganese sites.

PACS numbers: 64.70.Dv, 64.70.Rh, 71.45.Lr, 75.50.Cc

The ground state properties of the charge-ordered state in perovskite manganites is now well established [1–5]. Charge carriers in manganites introduced through the heterovalent ionic substitution could localize on the manganese sites and eventually become ordered in a striped pattern [6,7] at low temperatures. The antiferromagnetic charge-ordered state is a dominant phase competing with the ferromagnetic metallic ground state in the broad range of manganite phase space and has been the focus of many studies. One of the most intriguing phenomena associated with charge ordering is the collapse (or melting) of the ordered state under the influence of external perturbations such as magnetic field [8], pressure [9], or electromagnetic radiation [10]. The characteristics associated with the melting of the charge ordered state remain still largely unknown. The complex competition of several degrees of freedom such as charge, spin, lattice, and orbital could render it a very interesting system for the study of charge melting transition. Furthermore, the discrete nature of charge ordering on the regular manganese sites, which occurs as a result of strong coupling of the charge carriers and the lattice, can give rise to very different phase transition characteristics as compared to that in weakly coupled systems such as jelliumlike charge density waves [11,12]. In the charge density waves systems, the width of the modulation superlattice peak would increase rapidly near the transition temperature while the peak position which is determined by the nesting vector of the Fermi surface should remain largely unchanged (within a few percent) throughout the transition. This is consistent with the general notion that only the coherence length, not the periodicity, of the ordered phase is changing rapidly during the transition. In this Letter, we report an anomalous melting transition of charge ordering in the manganites which shows the periodicity of the charge-ordered phase changes dramatically by as much as 25% through the transition. Moreover, depending on the carrier concentration, some systems first go through a commensurate-incommensurate-like transition before the correlation length starts to change rapidly.

We have examined the melting characteristics of charge-ordered phase in the perovskite manganites of $(La, Ca)MnO_3$ and $(Pr, Ca)MnO_3$ as a function of temperature by electron diffraction and high resolution lattice images from transmission electron microscopy [7]. We used the polycrystalline samples prepared by standard solid state reaction and samples of $La_{1-x}Ca_xMnO_3$ and $Pr_{1-y}Ca_yMnO_3$ with various carrier concentrations of $x = 0.55$, 0.625, and 0.67, and $y = 0.5$ and 0.67 are chosen for the present study.

We first present the results obtained from the diffraction experiments. We measured the wave vector, $q = (2\pi/a_0)(\delta, 0, 0)$ and width γ (full width at half maximum) of the superlattice reflections due to charge ordering as a function of temperature. The intriguing melting behavior for various carrier concentrations is best demonstrated in these plots, and we find that they fall into two distinct types, I and II, as shown in Figs. 1 and 2, respectively. Specifically, melting characteristics for $x = 0.625$, 0.67 and $y = 0.67$ fall into type I, and that for $x = 0.55$ and $y = 0.5$ belong to type II. The differences between these two types will be elaborated later on. First of all, we note that the most fascinating feature shown in Figs. 1 and 2 is the dramatic change of the wave vector toward longer wavelength as the temperature is raised toward the charge-ordering transition temperature, T_{CO}. We note that the wave vectors shift to smaller values by as much as 25% through the transition.

We now look at these two types of melting more closely. As shown in Fig. 1, type-I melting of the charge-ordered state with carrier concentration close to $\frac{2}{3}$ is characterized by a simultaneous broadening and dispersion of modulation wave vector from $\delta \sim \frac{1}{3}$ to $\frac{1}{4}$ before the temperature reaches T_{CO}, as determined by transport measurements. At lower temperatures, the charge-ordering superlattice peak position remains unchanged ($\delta \sim \frac{1}{3}$) with its width limited by the experimental resolution (corresponds to ~50 nm in coherence length [13]). The peak width γ of the superlattice peaks is expressed in the unit of that measured from the fundamental Bragg reflections.

 0031-9007/99/83(23)/4792(4)$15.00 © 1999 The American Physical Society

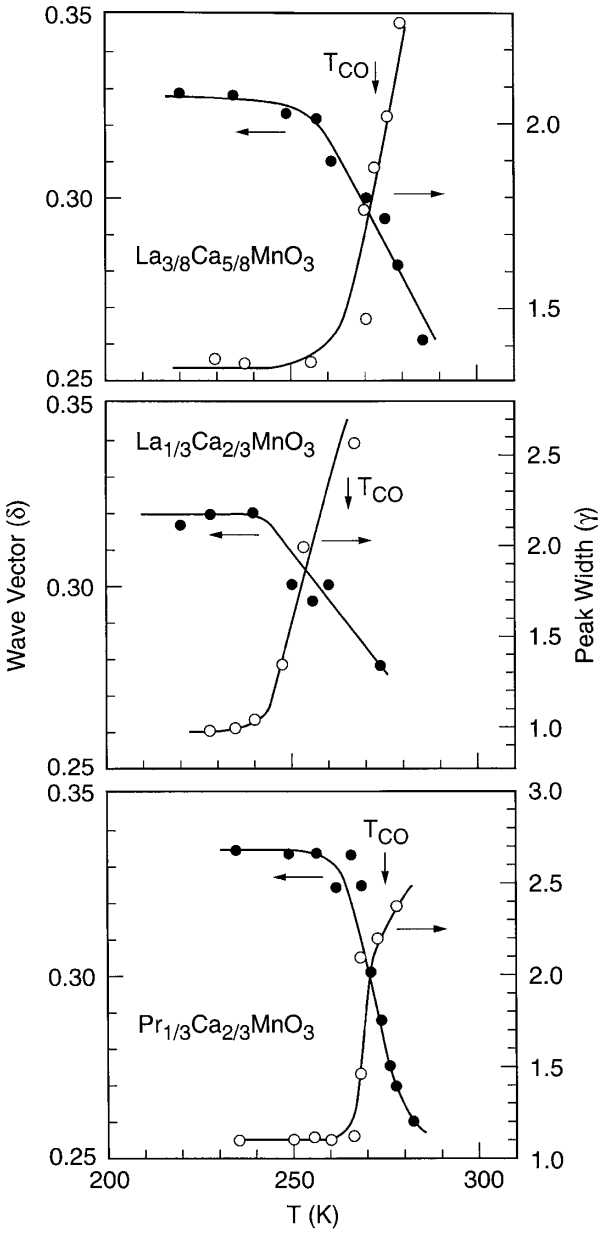

FIG. 1. Temperature dependence of wave vector (closed symbols) and peak width γ (open symbols) of charge-ordering superlattice reflections for $x = 0.625$ and 0.67 in $La_{1-x}Ca_xMnO_3$, and $y = 0.67$ in $Pr_{1-y}Ca_yMnO_3$. The simultaneous shift of the wave vector to longer wavelength positions and the rapid broadening of peak width near the charge-ordering transition temperature T_{CO} characterize the melting of charge-ordered phase in this case (type I).

The type-II melting characteristic (Fig. 2) with carrier concentration in the vicinity of $\frac{1}{2}$, on the other hand, is distinguished from type I by the presence of a commensurate-incommensurate (CM/IC)-like transition which precedes the actual melting. A similar CM/IC-like charge-ordering transition has also been reported in several previous studies of $Ln_{0.5}Ca_{0.5}MnO_3$ where Ln = Pr, Nd [14–16]. It is noted that the CM/IC transition takes place near the antiferromagnetic ordering temperature T_{AF} as indicated in

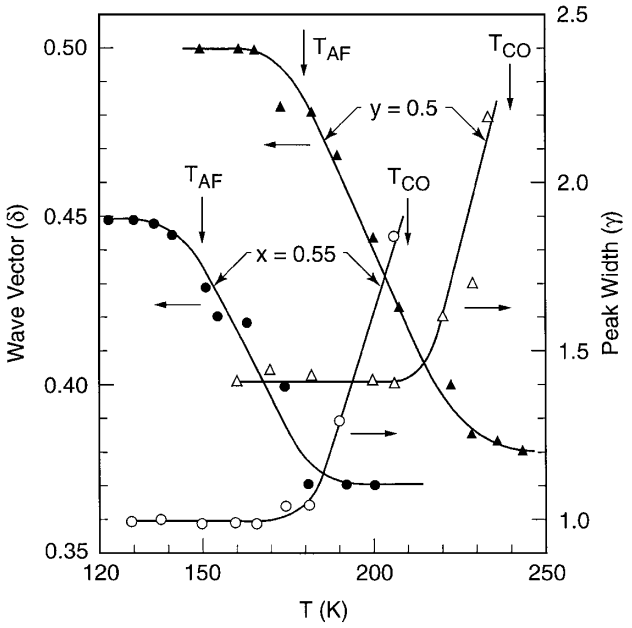

FIG. 2. Temperature dependence of wave vector (closed symbols) and peak width γ (open symbols) of charge-ordering superlattice reflections for $x = 0.55$ in $La_{1-x}Ca_xMnO_3$, and $y = 0.5$ in $Pr_{1-y}Ca_yMnO_3$. Melting of charge ordering is a two-stage process in this case (type II). It first goes through a commensurate-incommensurate-like transition near the antiferromagnetic ordering temperature (T_{AF}) before the melting actually takes place near T_{CO} where the peak width increases abruptly.

Fig. 2. In the temperature regime where this CM/IC-like transition occurs, the superlattice peak remains approximately as sharp as that for the low temperature CM phase within the resolution of our experimental conditions and, in the meantime, the modulation wave vector is dropping off rapidly (δ from $\sim\frac{1}{2}$ to $\frac{1}{3}$). The superlattice peak width starts to increase rapidly in this case around the temperatures where the decrease of wave vector begins to level off, similar to a normal modulated phase transition.

To understand this rapid dropoff of the wave vector in the type-I melting (Fig. 1), we have taken high resolution lattice images in this temperature regime. Recent high resolution studies of lattice images have shown that paired Jahn-Teller stripes (JTS) of the $Mn^{3+}O_6$ octahedra are the fundamental building blocks of the charge-ordered phase in the manganites, and the periodic array of these paired JTS gives rise to the superlattice reflections observed in the diffraction experiment [7]. Furthermore, it has been shown that the paired JTS in the charge-ordered phase adopts a few distinct periodicities such as 2, 3, and 4 times the orthorhombic cell parameter a_0 corresponding to the specific carrier concentrations of $x\,(y) = \frac{1}{2}$, $\frac{2}{3}$, and $\frac{3}{4}$, respectively [7]. For the type-I melting, our high resolution lattice images obtained at several different temperatures through the melting transition indicate that the nucleation of $2\pi/3$ phase shift boundaries across the paired JTS plays a crucial role in the melting

process. A high resolution lattice image showing the $2\pi/3$ phase shift boundaries obtained for $x = 0.67$ at 220 K is displayed in Fig. 3 where the paired lattice fringes with enhanced dark contrast has been previously ascribed to the paired JTS of the $Mn^{3+}O_6$ octahedra [7]. The inset of Fig. 3 shows a schematic of this phase shift boundary where the configuration of paired JTS on one side of the $2\pi/3$ phase boundary is shifted by a_0 relative to the other. It is noted that nucleation of the phase shift boundaries starts at temperatures much below T_{CO} where the correlation length of charge ordering remains large. As the temperature is raised toward T_{CO} more $2\pi/3$ phase boundaries are nucleated and the phase coherence length of paired $3a_0$ JTS start to get shorter. In the mean time, the charge-disordering process leads to a gradual breakup of the charge-ordered phase into a fine mixture of completely charge-disordered and partially charge-ordered clusters in the temperature regime where the superlattice peak has significantly broadened, as evidenced by the high resolution lattice images (not shown). The rapid size decrease of these charge-ordered clusters causes the superlattice peaks to broaden rapidly above 240 K. It is also noted that the presence of these $2\pi/3$ phase boundaries facilitates the formation of clusters with a larger separation of the paired stripes such as $4a_0$. This occurs near the end of the phase shift boundary where the paired JTS become in-phase again, as shown in the lower right corner of the inset of Fig. 3. The presence of the small clusters with $4a_0$ JTS near the ends of $2\pi/3$ phase shift boundaries, as indicated by the arrowheads, can also be seen clearly in Fig. 3. The rapid change of the wave vector between the two commensurate values from $\delta = \frac{1}{3}$ toward $\frac{1}{4}$ (see Fig. 1) through melting is a direct consequence of the fine random mixture of clusters of $3a_0$ and $4a_0$ paired JTS. Generally speaking, the separation of the paired JTS increases as the charge carriers become more disordered, and more $4a_0$-like paired JTS are formed as a result of the disordering process. Here we believe that the charge carriers in the paired JTS (in either $3a_0$ or $4a_0$ clusters) are still largely ordered (Mn^{3+}) and those localized on the manganese sites between them are disordered (with random mixture of Mn^{3+} and Mn^{4+}) to maintain the overall charge neutrality. Hence, the charge carriers are only partially ordered in these clusters. Further charge-disordering process would lead to the breakup of the paired JTS and gradually enlarge the size of the charge-disordered areas.

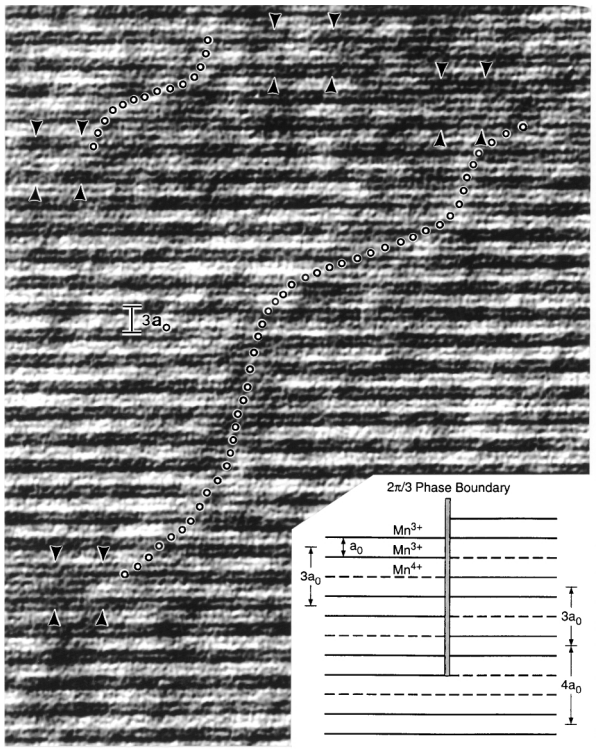

FIG. 3. High resolution lattice image taken at 220 K showing the initial stage of melting of charge ordering in $La_{0.33}Ca_{0.67}MnO_3$ by the nucleation of $2\pi/3$ phase boundaries highlighted with the curves outlined by the dotted circles. The presence of $4a_0$ JTS's near the ends of the phase boundaries is also indicated by the arrowheads. A schematic showing the $2\pi/3$ phase shift is also drawn in the inset, where paired Mn^{3+} stripes are denoted by solid lines and the dashed lines represent rows of Mn^{4+}. For clarity, only atomic rows of width a_0 (= 5.5 Å) spacing are shown in the inset with additional rows of Mn^{4+} being omitted.

Let us now look at the type-II melting for $x = 0.55$ and $y = 0.5$ as shown in Fig. 2. In this case, the melting of the charge-ordered state is preceded by the presence of a CM/IC-like transition in which the superlattice peaks exhibit no significant broadening. We note that the charge-ordered phase in this case, unlike the type-I melting shown in Fig. 1, is predominated by the presence of $2a_0$ paired JTS. In a previous study, it was found that charge ordering in $x = 0.5$ went through a similar CM/IC transition in a temperature regime where charge-ordered domains coexist with the ferromagnetic domains and the CM/IC transition coincides with the antiferromagnetic/ferromagnetic transition [4]. Most recently, it was found that the IC charge ordering in that case occurs as a result of incomplete d_{z^2} orbital ordering of the JTS [17] with the charge ordering remaining intact. The CM/IC transition as indicated in Fig. 2 has the same origin, as evidenced from our high resolution lattice images obtained in this temperature regime. This indicates that melting of the charge-ordered state in this case starts with d_{z^2} orbital disordering while maintaining the charge ordering. As temperature further increases, charge eventually becomes disordered and the superlattice peaks start to broaden rapidly.

It is noted that the charge ordering observed for the half-doped manganites with $x(y) = 0.5$ is special in which the ratio of Mn^{3+} and Mn^{4+} ions reaches the maximum value of one, and charge, spin, and orbital structure adopt a rigid and well-defined configuration as shown in Fig. 4 [1]. In this particular structure, charge and orbital ordered Mn^{3+} and Mn^{4+} ions form stable ferromagnetic

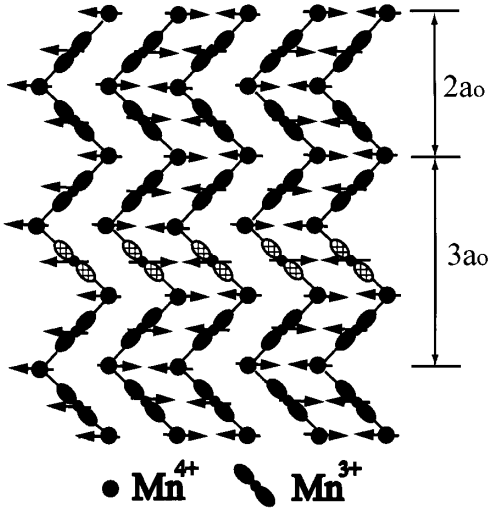

FIG. 4. Configuration of spin, charge, and d_{z^2} orbital ordering of the CE phase at half-doping in the a-b plane. Ferromagnetic zigzag chains of Mn^{3+} and Mn^{4+} ions are highlighted, and the antiferromagnetic coupling between the zigzag chains are also indicated by arrows. The close relationship between spin and orbital ordering is evident. Orbital disordering due to random d_{z^2} orbital orientation from a Mn^{3+} stripe (indicated by hatched orbitals) will break the periodic $2a_0$ JTS array and create a $3a_0$-like JTS cluster.

zigzag chains that are coupled antiferromagnetically. The ferromagnetic zigzag chains are intrinsically insulating due to a topological phase factor in the hopping, and the movement of e_g electrons (i.e., charge disordering) is severely inhibited in this case [18]. Hence, as the temperature is raised, orbital disordering takes place first while maintaining the charge ordering. This is consistent with the recent x-ray scattering results in similar systems where it was concluded that charge order fluctuations are more highly correlated than the orbital fluctuations [19]. It is clear from Fig. 4 that any orbital disorder on a Mn^{3+} site will affect the superexchange coupling with the four nearest Mn^{4+} spins. The fact that T_{AF} coincides with the CM/IC transition as indicated in Fig. 2 strongly supports the close link between orbital and spin ordering. The presence of orbital disordered Mn^{3+} stripes which act like discommensurations would locally break up the periodic $2a_0$ JTS configuration and lead to the appearance of $3a_0$-like JTS ordering (as indicated in Fig. 4) which then causes δ to change gradually from $\sim\frac{1}{2}$ toward $\frac{1}{3}$. For a carrier concentration around $\frac{2}{3}$ in which the charge ordering is predominated by the configuration of $3a_0$ JTS, e_g electrons in this case, without the rigid constraint found in the zigzag chains, could move more easily into the abundant Mn^{4+} sites separating the paired JTS as temperature increases and result in a simultaneous disordering of charge and orbital. Finally, we note that electron diffraction studies of charge ordering in both polycrystalline and single crystalline $Pr_{0.7}Ca_{0.3}MnO_3$, which also adopts the a modulation wave vector of $\delta = 0.5$ at low temperatures, do not show any temperature dependence of δ throughout the melting transition [20].

In conclusion, we have studied a new melting phenomenon of charge-ordered state in the perovskite manganites. The discrete nature of the charge ordering on the periodic Mn sites which gives rise to the discontinuous change of the modulation wave vector in the integral unit of lattice parameter is primarily responsible for the large shift of the ordering wave vector through the phase transition. This is distinctly different from that observed in another type of charge modulation such as the jelliumlike charge density waves (CDW) systems. In CDW systems, the close commensurability of the two competing length scales, namely, $1/(2k_F)$ of the Fermi surface and the lattice parameter, is a prerequisite for a CDW phase transition. This naturally leads to a much smaller change of the wave vector (within a few percent) through the phase transition [11,12]. Similar small variations of wave vector through the order-disorder transitions have also been reported in graphite-intercalated compounds [21,22].

We thank B. I. Shraiman and P. B. Littlewood for stimulating discussions.

[1] E. O. Wollan and W. C. Koehler, Phys. Rev. **100**, 545 (1955).
[2] J. B. Goodenough, Phys. Rev. **100**, 564 (1955).
[3] Y. Moritomo *et al.*, Phys. Rev. B **51**, 3297 (1995).
[4] C. H. Chen and S-W. Cheong, Phys. Rev. Lett. **76**, 4042 (1996).
[5] P. Ramirez *et al.*, Phys. Rev. Lett. **76**, 3188 (1996).
[6] C. H. Chen, S-W. Cheong, and H. Y. Hwang, J. Appl. Phys. **81**, 4326 (1997).
[7] S. Mori, C. H. Chen, and S-W. Cheong, Nature (London) **392**, 473 (1998).
[8] Y. Tomioka *et al.*, Phys. Rev. Lett. **74**, 5108 (1995).
[9] Y. Moritomo *et al.*, Phys. Rev. B **55**, 7549 (1997).
[10] V. Kiryukhin *et al.*, Nature (London) **386**, 813 (1997).
[11] R. M. Fleming *et al.*, Phys. Rev. Lett. **45**, 576 (1980).
[12] D. E. Moncton, J. D. Axe, and F. J. DiSalvo, Phys. Rev. B **16**, 801 (1977).
[13] Although the incident electron beam in our experiment is highly collimated and has a correlation length exceeding 400 nm, the present experimental condition with limited camera length and pixel size of the detector yields a much reduced correlation length ~50 nm.
[14] A. Barnabe *et al.*, J. Mater. Chem. **8**, 1405 (1998).
[15] A. Barnabe *et al.*, J. Appl. Phys. **84**, 5506 (1998).
[16] S. Mori *et al.*, Phys. Rev. B **59**, 13 573 (1999).
[17] S. Mori, C. H. Chen, and S-W. Cheong, Phys. Rev. Lett. **81**, 3972 (1998).
[18] J. van den Brink, G. Khaliullin, and D. Khomskii (unpublished).
[19] M. V. Zimmermann *et al.*, Bull. Am. Phys. Soc. **44**, 285 (1999).
[20] S. Mori and Y. Moritomo (unpublished).
[21] A. R. Kortan *et al.*, Phys. Rev. Lett. **49**, 1427 (1982).
[22] A. Erbil *et al.*, Phys. Rev. B **28**, 6329 (1983).